Research Article

ADVANCED PHOTONICS

# Resonantly driven nonlinear dynamics of soliton molecules in ultrafast fiber lasers

Defeng Zou,[a] Runmin Liu,[b] Yanqing Shi,[b] Aoyan Zhang,[a] Jialong Li,[a] Gina Jinna Chen,[a] Hong Dang,[a] Youjian Song,[b,*] Minglie Hu,[b,*] and Perry Ping Shum[a,c,*]

[a]Southern University of Science and Technology, State Key Laboratory of Optical Fiber and Cable Manufacture Technology, Guangdong Key Laboratory of Integrated Optoelectronics Intellisense, Department of EEE, Shenzhen, China
[b]Tianjin University, School of Precision Instruments and Opto-electronics Engineering, Ultrafast Laser Laboratory, State Key Laboratory of Precision Measurement Technology and Instruments, Tianjin, China
[c]Pengcheng Laboratory, Shenzhen, China

**Abstract.** Recent years have seen significant advances in the study of dissipative soliton molecules in ultrafast lasers, driven by their remarkable connections to a wide range of physical systems. However, understanding and controlling the underlying physics of soliton molecules remain elusive due to the absence of a universal physical model that adequately describes intramolecular motion. We demonstrate that resonant excitation generates breather soliton molecules, with their resonance susceptibility exhibiting high amplitude-driven operations that can be well understood within the framework of the Duffing model. Harnessing powerful experiment techniques and detailed numerical simulations, we reveal the fundamental resonant mode within intrapulse separation constrained to the 100 fs level as well as the presence of the subharmonic and overtones. Additionally, we observe chaotic dynamics arising from the multiple-frequency nonlinear interactions in a strongly dissipative regime. Our work provides a perspective on the complex interactions of dissipative optical solitons through the lens of nonlinear physics. This approach offers a simple test bed for complex nonlinear physics research, with ultrafine scanning of temporal separations of ultrashort laser pulses demonstrating significant potential for applications requiring high detection sensitivity.

Keywords: nonlinear dynamics; resonant excitation; soliton molecules; balanced optical cross correlation; ultrafast lasers; Duffing model.

Received Sep. 24, 2024; revised manuscript received Nov. 20, 2024; accepted for publication Dec. 24, 2024; published online Feb. 7, 2025.



[DOI: 10.1117/1.AP.7.1.016005]

## 1 Introduction

Nonlinearity is an intrinsic characteristic of dynamic systems, driving research across a broad range of disciplines, from physics and mechanical engineering to biology, and spanning scales from macroscopic to microscopic.[1,2] Self-assembly and emergent many-body dynamics driven by nonlinear physics represent a frontier in modern science. These areas explore how complex systems—composed of multiple interacting components—exhibit behaviors due to intrinsic nonlinearity in their governing mechanisms.[3–5] Researchers have used nonlinear differential equations to model and elucidate these systems for decades, achieving significant insights into their behavior.[6] For instance, the Lorenz equations have been pivotal in characterizing atmospheric convection patterns, enhancing our understanding of weather systems and the inherent limits of meteorological predictability. The study of nonlinear dynamics is not only crucial for fundamental research but also intimately connected with practical applications, establishing it as a cornerstone in the study of various dynamical systems ranging from simple pendulums to micro/nanoresonators and nonlinear metamaterials.[7,8] For instance, employing nonlinear techniques for fine-tuning the damping of nanoresonators holds promise for enhancing their capabilities in force microscopy and quantum

*Address all correspondence to Youjian Song, yjsong@tju.edu.cn; Minglie Hu, huminglie@tju.edu.cn; Perry Ping Shum, shum@ieee.org

information processing.[9] In optics, nonlinear processes are intimately connected with supercontinuum generation,[10] pattern formation,[11–14] and attosecond laser pulses[15] and are essential for optical frequency combs arising from Kerr effects and quadratic nonlinearities in microresonators.[16–18]

Passively mode-locked fiber lasers serve as ideal platforms for studying nonlinear physics, primarily due to two key factors. First, the ultrashort pulse sequences they generate possess extremely high peak powers, accentuating nonlinear effects, such as dissipative Talbot effects and modulation instability.[19,20] Second, interactions between these ultrashort pulses can lead to the formation of compact soliton molecules, a phenomenon that, owing to its rich internal dynamics, has recently garnered significant attention for its profound parallels with related fields such as fluid dynamics and complex network systems.[21–30] Typically, intramolecular dynamical changes are subtle and difficult to discern, necessitating advanced detection techniques, such as dispersive Fourier transform,[31–35] which can infer intramolecular degrees of freedom, like relative phase shifts from single-shot spectra or balanced optical cross correlation (BOC), which offers subfemtosecond temporal resolution for detecting variations in intrapulse separation.[36,37]

Existing studies on soliton molecule dynamics, such as the buildup process and spontaneous oscillations,[38–41] have primarily focused on the adjustment of laser parameters. There has been limited investigation into the deterministic control or modulation of soliton molecule dynamics through external driving mechanisms. This aspect is crucial, as achieving deterministic driving over soliton molecule states is fundamental for their application in all-optical communication,[42–44] encoding,[45] and storage.[46] More importantly, it offers the opportunity to probe the underlying nature of intramolecular dynamical systems by analyzing the nonlinear responses driven by external modulation. Recent studies on bichromatically pumped Kerr resonators have revealed composite solitons exhibiting transient resonances, underscoring the eigenfrequencies inherent in dissipative soliton dynamics.[47] However, it remains elusive whether nonlinear intramolecular dynamics in passively mode-locked fiber lasers can be externally driven, and the physical mechanisms involved are yet to be fully understood and are poorly matched with existing physical models.

In this work, we venture into an unexplored regime of soliton molecule dynamics, where the concept of driven damped resonators is applied, for the first time to our knowledge, to intramolecular systems in ultrafast lasers. Through experimental observations and simulations, we reveal the susceptibility of Fano-type resonance in intrapulse separation, with resonance amplitudes confined to sub-100 fs scales, facilitated by the effective coupling between external modulation and laser gain. Here, we address a crucial challenge: attaining precise modulation of soliton molecule dynamics via external cavity injection to explore intramolecular nonlinear physics while preserving the original laser parameters and bound states structure under stable mode-locking conditions. We further confirm that resonance susceptibility exhibits a strong dependence on the amplitude of motion governed by nonlinear rather than linear dynamics. We uncover the Duffing-type nonlinearity in dissipative soliton interactions by modeling the backbone curve using a driven Duffing equation. This mechanism, tied to an anharmonic binding potential, enables direct probing of the overtones/subharmonic, even chaotic responses within intramolecular dynamics.

## 2 Results

### 2.1 Experimental Setup

Figure 1 illustrates the laser configuration and detection system employed in investigating the nonlinear response of soliton molecules. A typical dispersion-managed passively mode-locked fiber laser is used to generate multipulse states, utilizing a mode-locking mechanism based on nonlinear polarization rotation (NPR). A 980/1550 nm wavelength division multiplexer connects the laser diode and the gain fiber (Liekki Er 110-4/125), efficiently coupling the pump light into the laser cavity. The free-space components consist of three wave plates, an isolator, and a polarizing beam splitter, utilized, respectively, for polarization adjustment, ensuring unidirectional light transmission, and outputting the laser signals. The laser operates in a near-zero, slightly negative dispersion regime, with a net dispersion of approximately $-0.07$ ps$^2$. Due to the intensity-dependent loss introduced by NPR, adjusting the gain strength and polarization state offers a convenient and flexible method for tuning the laser into the desired mode-locking regime. Soliton molecules demonstrate robust performance and stability in this regime, even under external injection. The external driving signal is injected through an optical coupler. A continuous wave (Santec TSL-550) signal is initially amplified using a custom-built erbium-doped fiber amplifier. The amplified signal is then modulated by an electro-optic modulator (Conquer KG-AM-15-2.5G) and inscribed with a sweeping driving signal using a function generator. This signal is subsequently coupled into the cavity through the coupler.

The mode-locked pulse train, optical spectrum, and radio-frequency (RF) spectrum of the laser repetition rate are characterized by an oscilloscope (Agilent Infinium), optical spectrum analyzer (Yokogawa AQ63700), and electrical spectrum analyzer (Rigol DSA815), respectively. A flippable mirror is utilized to direct the laser output into the BOC system [see Fig. 1(c)], enabling the detection of intramolecular dynamics. Scanning the movable mirror in one arm of the Michelson interferometer results in an S-shaped curve, with the linear region (marked in green) corresponding to the zero crossing. For details on the principle and adjustment of the BOC system, refer to our paper,[48] in which the subfemtosecond resolution of the BOC technology was experimentally demonstrated. By implementing precise control techniques and high-resolution real-time observation methods, we have experimentally observed the resonant response of pulse separations within soliton molecules. The susceptibility of this response exhibits a pronounced shift with increasing resonance strength, providing deep insights into the anharmonic potential governing the interactions between optical solitons [Fig. 1(d)]. We achieved an excellent fit of the resonance frequency shift using the Duffing equation, indicating that Duffing-type nonlinearity plays a crucial role in the nonlinear resonant response within the molecule when the soliton molecule is analogized to a driven damped oscillator [Fig. 1(e)]. Furthermore, we successfully trigger a subharmonic response away from the fundamental resonance frequency. Under appropriate driving strengths, the subharmonic and chaotic response can dominate intramolecular dynamics, reflecting the multiple thresholds required for different oscillating modes in soliton interactions [Fig. 1(f)].

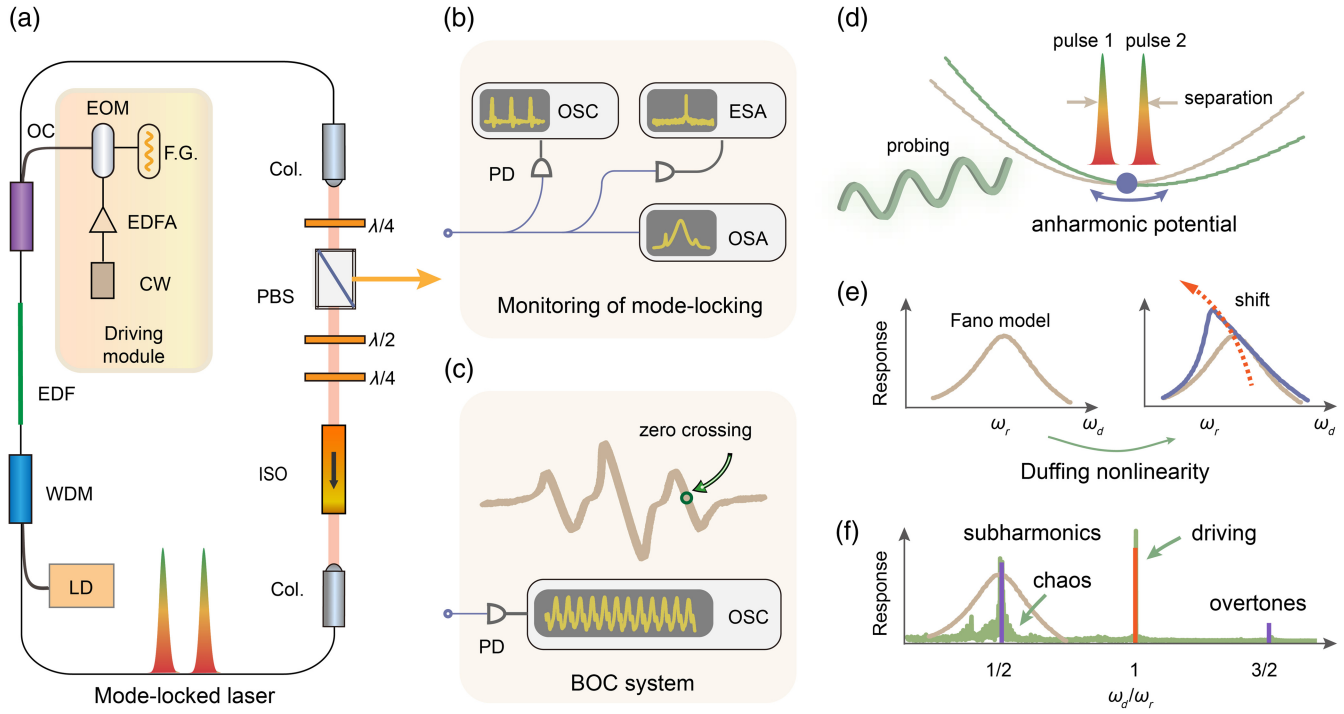


**Fig. 1** Concept and demonstration of resonant excitation of nonlinear dynamics of soliton molecules. (a) Experimental setup of the mode-locked fiber laser: LD, laser diode; WDM, wavelength division multiplexer; EDF, Er-doped fiber; OC, output coupler; Col., collimator; PBS, polarization beam splitter; QWP, quarter-wave plate; HWP, half-wave plate; ISO, isolator. Driving module: CW, continuous wave; EDFA, erbium-doped fiber amplifier; F.G., function generator; and EOM, electro-optic modulator. (b) Mode-locking status monitoring module: PD, photodiode; OSC, oscilloscope; ESA, electrical spectrum analyzer; OSA, optical spectrum analyzer. (c) BOC system used to detect variations in intrapulse separation. (d) The resonant excitation induces forced oscillations in the intrapulse separation, implying that the system periodically traverses different positions on the anharmonic potential curve under external driving. (e) Schematic of resonance frequency shifts induced by Duffing-type nonlinearity. (f) Schematic of harmonic/subharmonic responses and chaotic dynamics. $\omega_d$: driving frequency; $\omega_r$: eigenfrequency.

### *2.2 Experimental Resonant Excitation of Soliton Molecules*

Stationary soliton molecules exhibiting constant intrapulse separation are realized by adjusting the pump strength within an appropriate range, specifically ∼520 to 600 mA. The optical spectrum corresponding to the mode-locked state at a pump current of 530 mA, shown in Fig. 2(a), reveals pronounced interference fringe patterns indicative of the established bound-soliton structure. The fringe period of ∼2.32 nm corresponds to an intrapulse separation of about 3.5 ps, with a pulse duration of ∼300 fs. The rapid intramolecular oscillations exceed the mechanical scanning speed of the spectrometer, resulting in an averaging of the fast dynamics in the output spectrum. Nevertheless, the stability of the intrapulse separation can still be inferred from the fringe visibility, which reaches 100%. In contrast, the intrapulse separation varies over time for oscillating or chaotic soliton molecules, significantly reducing the modulation depth of the interference fringes.[31,41] Figure 2(b) illustrates the pulse sequence, where the interval between consecutive pulses is measured to be 22 ns, corresponding to the round-trip time within the laser cavity. This interval aligns with a laser repetition frequency of ∼45 MHz.

Next, we proceed with the resonant excitation of the intrapulse separation in soliton molecules. The stationary state with constant separation depicted in Fig. 2(a) is employed as the initial state. We apply a logarithmic frequency-swept intensity-modulated sinusoidal signal with a central wavelength set within the gain spectrum of the Er:fiber at 1530 nm, and an average power of ∼3 mW. Empirically, when the injected power exceeds 5 mW, the mode-locked state is readily disrupted. The sweep period is set to 50 ms, covering a frequency range from 100 Hz to 10 MHz. Representative responses of the intramolecular separation over several periods are captured in Fig. 2(c), in which the amplitude of the pulse separation response varies with changes in the driving frequency. A clear correlation between the response amplitude and the driving frequency is observed. The response of intramolecular separation peaks at a specific driving frequency, where the maximum amplitude approaches 100 fs. To explore the pulse energy variation during the frequency sweep, a 10 MHz low-pass filter was used to isolate low-frequency energy fluctuations while filtering out the high-frequency pulse sequences. The brown curve in Fig. 2(c) shows that the pulse energy exhibits a consistent response pattern with the intrapulse separation.

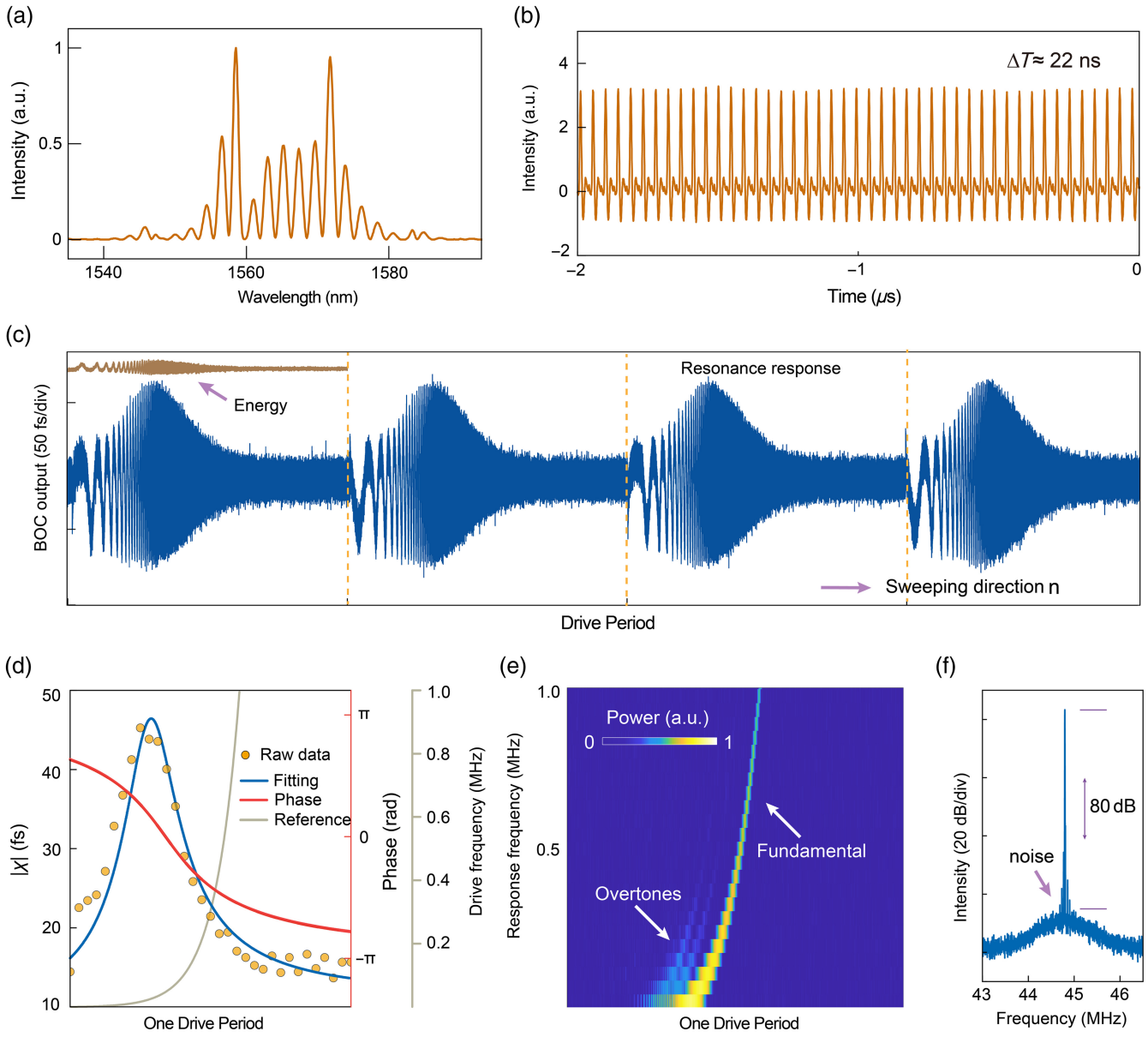


**Fig. 2** Experimental measurements of the mode-locked state and resonant excitation of soliton molecules. (a) Optical spectrum and (b) pulse sequence. (c) Response of intrapulse separation under external driving detected by the BOC system. Resonant pulse energy for a driving period is also shown as the brown curve. (d) Resonant susceptibility $\chi(f)$ with Fano line shape fitting, where the red curve represents phase evolution. The driving frequency is also presented as the gray curve. (e) The two-dimensional spectra extracted from the short-time Fourier transform of (c) display fundamental response and overtones. (f) RF spectrum of the laser repetition rate under external driving.

The frequency-dependent susceptibility $\chi(f)$ of the change in intrapulse separation can be simply evaluated from the envelope of the BOC data across the entire frequency sweep. The susceptibility function facilitates the fitting of the resonance curve, thereby evaluating the resonance frequency. As depicted in Fig. 2(d), the blue curve shows the Fano fit applied to the experimental data (scatter points).[49] For further clarity, the driving frequency over a single period is also plotted (gray curve). From this analysis, we estimate the resonance frequency to be ~5.2 kHz. We observe a slight asymmetry in the susceptibility curve, which can be attributed to the presence of a nonresonant background. The nonresonant background, typically associated with continuum states, has a complex origin that may include instantaneous Kerr nonlinearity or an inhomogeneous noise floor induced by laser gain depletion.[50] Additionally, the phase extracted from the susceptibility curve reveals a shift of approximately $\pi$ across the entire resonance region (red curve). Figure 2(e) shows the short-time Fourier transform of a single resonance period of the BOC signal depicted in Fig. 2(c). Along with the fundamental resonance mode, the transform reveals

prominent overtones, including the second and third harmonics. The observation of these harmonics underscores the nonlinear characteristics of the dynamical system (soliton molecules here), which are also evident in other nonlinear systems, such as optomechanical oscillators.[51] In addition, we assess the mode-locking stability of soliton molecules during the intrapulse resonance. As depicted in Fig. 2(f), while applying the external signal markedly raises the noise baseline of the RF spectrum of the laser repetition rate, the signal-to-noise ratio remains above 80 dB. This indicates that the mode locking is highly stable.

### 2.3 Simulation Results

To verify the generality of the intramolecular resonance response and to uncover its deeper physical insights, we conduct numerical simulations using the scalar generalized nonlinear Schrödinger equation. [52] This equation incorporates fundamental physical effects within the laser cavity, including dispersion, self-phase modulation, finite gain bandwidth, and saturable gain. The key components of the model include an EDF as the gain fiber, two segments of single-mode fiber, and an output coupler. A fast saturable absorber model is employed to achieve the mode locking. The gain dynamics are controlled via round-trip—varying modulation of the small-signal gain coefficient $g_0 = g_{0s}(1 + M_f \sin(2\pi f R_{ts}))$, where $R_{ts}$ is the laser round trips and $g_{0s}$ refers to the small-signal gain coefficient corresponding to the initial stationary soliton molecules. $M_f$ is the modulation depth, and $f$ is the modulating frequency. Given that the simulation model assumes an ideal environment without accounting for the diverse sources of experimental noise, the resonance response can be realized at a low driving strength. For a detailed description of the simulation model for the ultrafast fiber laser, refer to Sec. A in the Supplementary Material.

Figure 3(a) shows the resonant response of the internal dynamics of soliton molecules at a modulation depth of 0.1%. Both the intrapulse separation and pulse energy exhibit clear resonant responses, which are in high agreement with the experimental results. Additionally, we examine the consistency of energy fluctuations for each pulse within the molecule during the resonance process. The inset shows that pulses 1 and 2 always experience synchronized energy variations. This indicates that the resonant response of the intramolecular system is not directly but rather indirectly related to the gain dynamics, reflecting an intrinsic nonlinear dynamical behavior. Perturbations in gain simultaneously affect the energies of both pulses, leading to changes in the underlying interaction potential and ultimately driving the resonance in the intrapulse separation. Figure 3(b) shows the corresponding spectral evolution with the orange-highlighted spectral profile. Away from the resonance frequency, spectral changes are nearly imperceptible. However, the spectrum undergoes clear periodic broadening and narrowing at the resonance region, exhibiting a distinctive breathing pattern. Following the experimental procedure, we apply a short-time Fourier transform to the response of the intrapulse separation, revealing a distinct second-harmonic response in Fig. 3(c). Higher-order harmonics, such as third-harmonic observed in the experiment, do not manifest due to the minimal driving modulation depth of only 0.1%. In line with the experimental results, the susceptibility in Fig. 3(d) also follows a Fano line shape with a phase shift of $\pi$. A prominent resonance peak is evaluated at ~5.8 MHz. In Fig. 3(e), we stop the frequency sweeping and stabilize the driving at the resonance frequency to monitor the transition of the intrapulse separation from a constant to oscillatory behavior. This transition occurs rapidly, within fewer than 100 round trips, and demonstrates remarkable reproducibility and stability.

As a further note, it is inherently interesting to observe that the resonance frequency is significantly higher than the experimentally observed values. In our previous work, we applied semiclassical noise theory to analyze stationary soliton molecules under the influence of amplified spontaneous emission, focusing on their quantum noise limit.[36] Although this was not explicitly highlighted, we indeed observe a characteristic eigenfrequency, which was designated as the cutoff frequency. Our prior experimental and simulation results demonstrated a pronounced correlation between this eigenfrequency and the intrapulse separation, which well supports the divergence observed between current experimental and simulation results: a longer separation, ranging from a few picoseconds to several tens of picoseconds, corresponds to a significantly lower cutoff frequency, which can drop to just a few kilohertz or even below 1 kHz. Conversely, a shorter separation (0.9 ps in the simulation) corresponds to a much higher cutoff frequency reaching several megahertz. Here, our simulation results are not intended for quantitative comparison with the experiment but are designed to qualitatively support the general resonance dynamics within soliton molecule dynamics.

After successfully validating the experimentally observed resonance dynamics of intrapulse separation, we further investigate the evolution of the resonance response under strong driving conditions in the simulation model. This scenario is particularly challenging to achieve in experimental settings due to the detrimental effect of experimental noise, which diminishes the robustness of soliton molecules to resist intense external perturbations. As illustrated in Fig. 4(a), the waveforms of the susceptibilities remain stable across varying driving strengths. The peak amplitude increases with driving strengths, with its linear growth trend depicted in Fig. 4(b). Notably, a significant shift in the resonance frequency is observed in Fig. 4(a), which indicates a strong dependence of the resonance characteristics on the driving strength. Such behavior is interpreted within the framework of nonlinear physics and is associated explicitly with the softening effect induced by Duffing-type nonlinearity.[3]

We extract the resonance frequencies and plot them on the vertical axis against the maximum amplitudes on the horizontal axis to construct the backbone curve. The result highlights a distinct critical amplitude, beyond which the system, driven with an amplitude significantly exceeding typical operational conditions, manifests pronounced nonlinear effects, marking the dominance of high amplitude-driven operations. As depicted in Fig. 4(c), the resonance frequency decreases with increasing response amplitude, exhibiting a behavior that significantly deviates from a linear fitting (dashed black line). We model this by solving the amplitude for a driven Duffing oscillator,

$$\mathrm{d}^2x/\mathrm{d}t^2 + 2\zeta\omega_0 \mathrm{d}x/\mathrm{d}t + \omega_0^2 x + \frac{k_3}{m_{\mathrm{eff}}}x^3 = \frac{F}{m_{\mathrm{eff}}}, \tag{1}$$

where $x$ represents the displacement corresponding to the resonant amplitude of the intrapulse separation. $m_{\mathrm{eff}}$ is the effective modal mass, $\omega_0$ is the eigenfrequency, and $\zeta$ is the linear damping coefficient. The external driving term is $F = F_0 \cos(\omega t)$. The nonlinear term $k_3 x^3$ introduces an amplitude-dependent

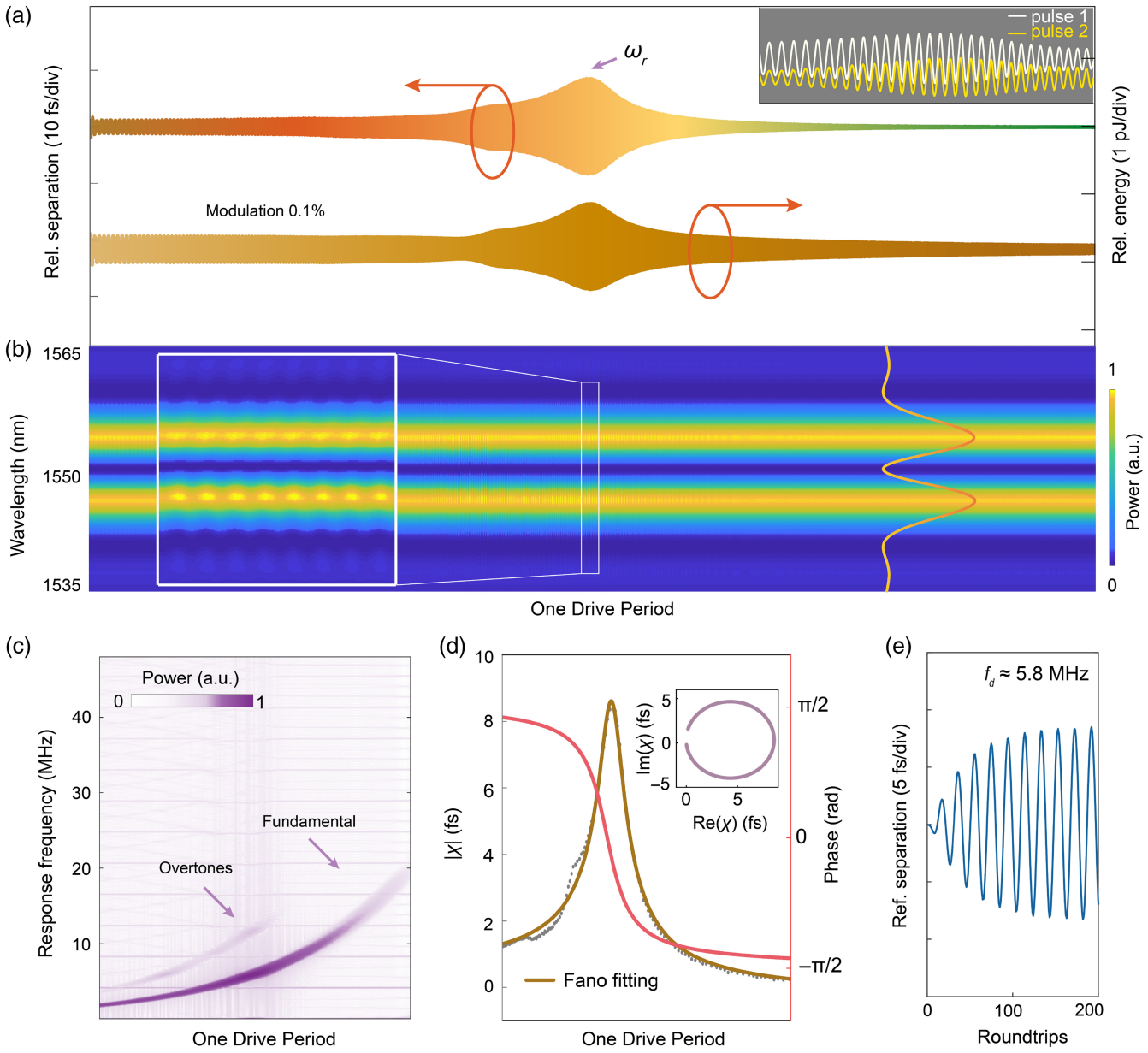


**Fig. 3** Simulation of resonant excitation of soliton molecules under 0.1% external driving. (a) Resonance response of intrapulse separation, with the pulse energy response shown by the brown curve. The inset illustrates the energy variation of each pulse within the molecule, highlighting a high consistency. (b) Spectral evolution under frequency sweeping, with the white box highlighting an enlarged view at the resonance region. The orange curve represents the single-shot spectra. (c) Two-dimensional spectra extracted from the short-time Fourier transform of intrapulse separation in (a). (d) Resonant susceptibility $\chi(f)$ with Fano line shape fitting, where the red curve represents phase evolution. Inset: the corresponding Nyquist plot in the complex plane. (e) Transient behavior of intrapulse separation transitioning from no driving to stable forced oscillations, with the driving frequency fixed at 5.8 MHz.

frequency shift, resulting in the bending of the backbone curve as the amplitude increases. Following the derivation approach outlined in Ref. 53, the backbone curve of Eq. (1) can be derived as

$$\Omega = \omega_0 + \frac{3k_3}{8m_{\text{eff}}\omega_0} r^2. \tag{2}$$

Equation (2) is used to fit the backbone curve of the resonant soliton molecules, achieving a high degree of consistency, as indicated by a fitting $R^2$ value of 0.97 [green curve in Fig. 4(c)]. For detailed descriptions of the driven Duffing oscillator and the fitting of the backbone curve of soliton molecules, refer to Sec. B in the Supplementary Material. Additionally, we apply Fano fitting to all susceptibility curves in Fig. 4(a).

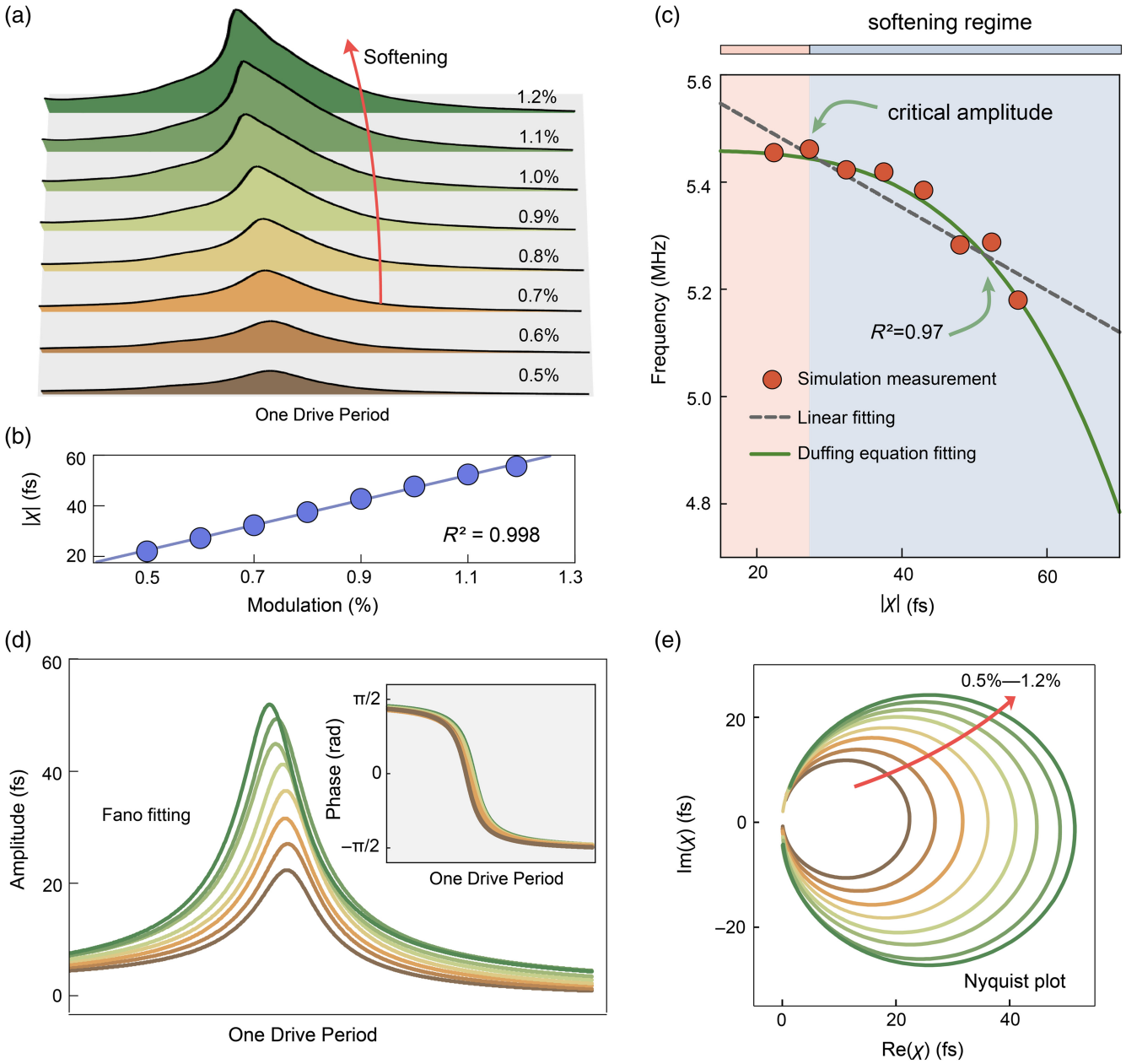


**Fig. 4** Simulation of resonant excitation of soliton molecules under driving strengths ranging from 0.5% to 1.2%. (a) Resonant susceptibility $\chi(f)$. (b) Trend of maximum response amplitude and its linear fit. (c) Backbone curve with linear and Duffing equation fitting. (d) Fano fittings of the resonant susceptibility. Inset: phase evolution. (e) Nyquist plots in the complex plane.

Although the asymmetry of the curves becomes more pronounced with increased driving, the fits in Fig. 4(d) remain reasonable, accompanied by uniform phase curves [inset in Fig. 4(d)] and Nyquist plots [Fig. 4(e)] consistent with the weak driving scenario in Fig. 3(d), as well as the experimental results in Fig. 2(d).

Next, we shift our focus to the frequency range far from the fundamental resonance mode. This approach allows for significantly stronger driving without destabilizing the binding structure of molecules due to excessive resonance effects. We set the driving frequency to 10 MHz, approximately twice the eigenfrequency, and increase the driving strength from 5% to 13%. The resulting separation response is shown in Fig. 5(a), with its short-time Fourier transforms presented in Fig. 5(b). Within the driving strength range of 5% to 8%, the response amplitude increases smoothly with increasing driving strength. However, when the driving strength surpasses 8%, a distinct critical behavior is observed, characterized by a rather sharply defined order-of-magnitude increase in the amplitude and the emergence of a subharmonic frequency at 5 MHz. This behavior indicates that the system has crossed a critical subharmonic threshold, where second-order nonlinear interactions become sufficiently strong to initiate and sustain oscillations at half the driving frequency (5 MHz). Below this threshold, the driving

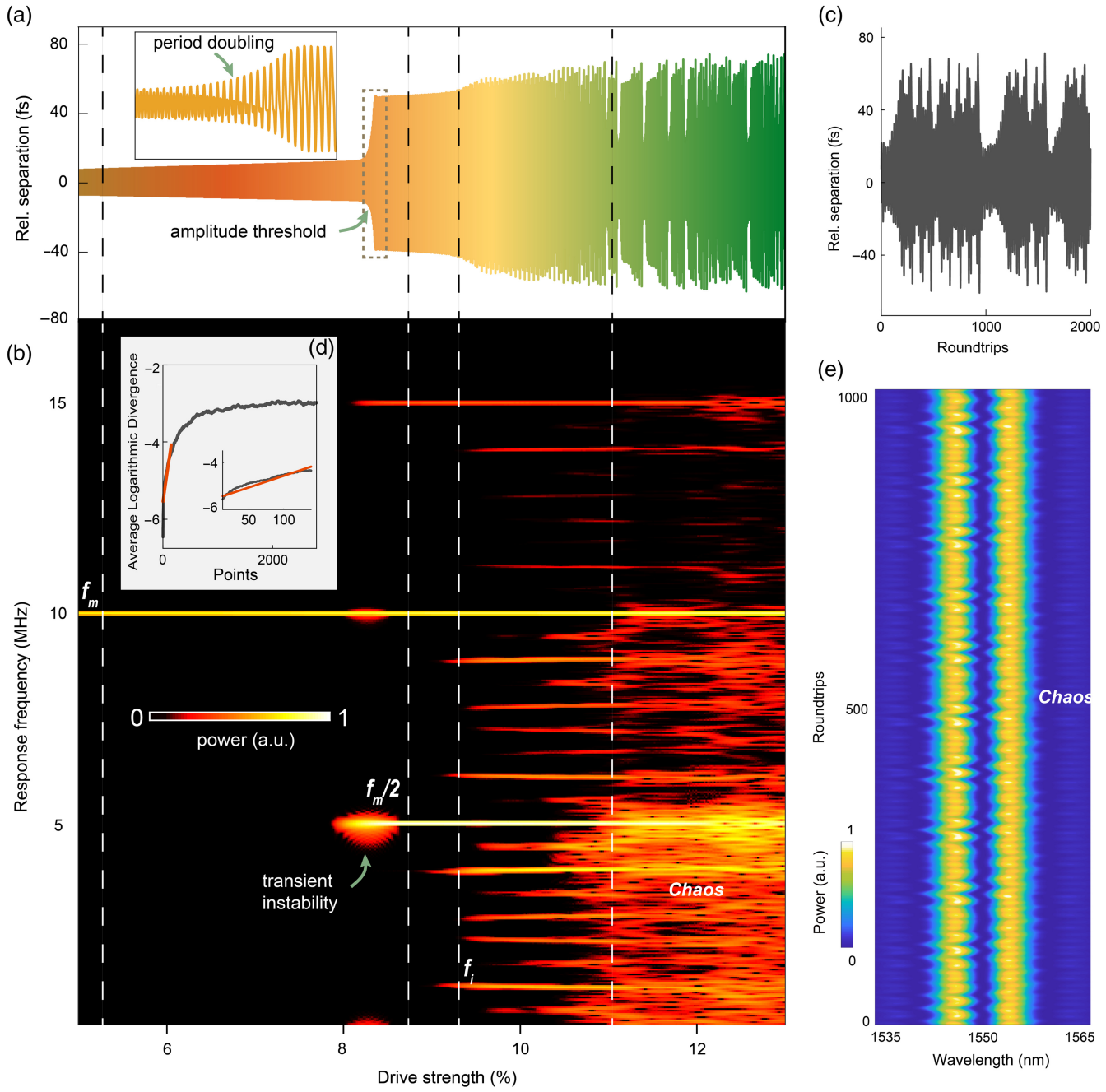


**Fig. 5** Subharmonic response and deterministic route to intramolecular chaos obtained by sweeping driving strength far from the fundamental resonance region. (a) Intrapulse separation response. Inset: an enlarged view of the boxed region shows a distinct amplitude threshold, above which the subharmonic response dominates. The transition from the fundamental to subharmonic modes manifests period-doubling bifurcation characteristics. (b) Two-dimensional spectra extracted from the short-time Fourier transform of intrapulse separation in (a). The dashed lines spanning (a) and (b) indicate the system's operation across different modes. (c) Chaotic separation response at a fixed driving strength of 11%. (d) Lyapunov exponent analysis of intrapulse separation in (c). Inset: enlarged view of the linear region. (e) Chaotic spectral evolution.

force at 10 MHz primarily excites the fundamental mode, with energy transfer to other modes, including the subharmonic, being too weak to overcome critical damping. However, as the driving amplitude surpasses the threshold, the nonlinear coupling between the fundamental and subharmonic modes intensifies, leading to more efficient energy transfer. This results in a bifurcation in the separation response, where the subharmonic mode not only emerges but stabilizes, increasing in amplitude until it can coexist with or even dominate the oscillation.[54]

We observe extreme sensitivity at the bifurcation point in the full-record spectrogram, where pronounced transient instabilities emerge and dissipate. These transient processes are frequently accompanied by spontaneous self-modulation and occur during transitions between various oscillation modes.[55] As we further increase the driving strength to 9%, beyond the subharmonic threshold, an additional frequency component $f_i$ at ∼1.1 MHz emerges, incommensurate with the driving frequency. This signals the onset of quasi-periodic dynamics, characterized by a two-dimensional torus in phase space.[56] In nonlinear systems, quasi-periodic dynamics are intrinsically linked to the emergence of chaos, manifested through irregular and unpredictable oscillations, as demonstrated in our observations of soliton molecules. This chaotic regime emerges when the driving strength surpasses ∼11%, where the intramolecular system exhibits increasingly complex and erratic behavior. As shown in the spectrogram, the distinct oscillation frequency peaks resulting from nonlinear mode coupling disappear, and the noise floor significantly increases, providing qualitative evidence for the presence of chaos.

To provide quantitative evidence of chaos, we perform a Lyapunov exponent analysis on the response signal of intrapulse separation obtained with a fixed driving strength of 11%. Lyapunov exponents quantify the rate of exponential divergence between nearby trajectories in phase space, which is essential for identifying chaotic dynamics. As shown in Fig. 5(d), the average initial logarithmic divergence of neighboring trajectories follows a linear trend, confirming the presence of chaotic dynamics through positive maximal Lyapunov exponents.[57] The enlarged view of the linear region is shown in the inset. Finally, the spectral evolution corresponding to Fig. 5(c) is presented in Fig. 5(e), revealing pronounced spectral fluctuations accompanied by oscillations in the interference fringes. These oscillations deviate from the regular breathing periodicity characteristic of breather molecules,[39] instead exhibiting erratic and unpredictable oscillatory behavior. We note that the emergence of chaos here does not follow the classic, well-defined routes, but rather involves a new modulated subharmonic route characterized by a "subharmonic–quasi-periodic–chaotic" sequence, highlighting an intrinsic complexity analogous to that of low-dimensional nonlinear systems, as observed in dissipative solitons.[58,59]

## 3 Discussion

Our work casts light on a series of unresolved questions about soliton molecule dynamics. First, what are the eigenfrequencies involved in intramolecular dynamics? Our combined experimental and simulation efforts reveal key aspects of the intramolecular resonance mechanism within the framework of nonlinear dynamics. Stationary soliton molecules exhibit strong internal damping that exceeds the critical threshold, thereby suppressing spontaneous oscillatory behavior such as limit-cycle dynamics. However, supercritical bifurcations occur when driven externally with sufficient strength, leading to sustained forced oscillations. Upon cessation of the driving force, the system naturally returns to a fixed-point attractor, characterized by stable intrapulse separation, a behavior consistent with overdamped systems. This reversion is confirmed by gradually reducing the driving signal to zero. These eigenfrequencies are intrinsic to the solitonic bound state and are solely determined by the characteristics of the underlying binding potential, such as the damping properties. Although they can be excited through modulation of the laser gain, they do not directly depend on gain dynamics. Similar observations have been confirmed in composite dissipative Kerr solitons within Kerr resonators.[47]

Second, how can soliton molecules be driven to achieve resonance in fiber lasers? Previous works have developed pump current modulation strategies that have been successfully applied to switching between discrete soliton doublet states and phase-tailored assembly.[44,45] However, considering that the resonance response of the intrapulse separation is minimal (<100 fs), it is highly likely to be obscured by the inherent bias introduced by the laser transfer function when employing pump current modulation techniques. Here, we utilize an efficient extrinsic coupling mechanism based on gain competition between the modulated signal and soliton molecules. This all-optical strategy facilitates precise resonance excitation on sub-100 fs timescales over a wide frequency range from kilohertz to megahertz. Notably, one potential disadvantage may be that such external driving is independent of the laser system and, therefore, requires more empirical evaluation of the driving tolerance limits, specifically balancing adequate drive while maintaining the mode locking. Additionally, by directing the injected light opposite to the lasing mode, with the intracavity optical isolator ensuring a single pass through the $Er^{3+}$ fiber, gain competition between the injection signal and the lasing mode in the gain medium enables efficient modulation of the laser gain, overcoming the slow gain recovery limitation and achieving megahertz-level driving speed.

Last, what are the manifestations of soliton nonlinear interactions? Here, we observe a range of intriguing nonlinear phenomena near and far from the fundamental resonance region, including resonance frequency shifts, which exhibit a universal nature that could be characterized using the Duffing model. Additionally, we explore the critical subharmonic response dynamics across varying drive strengths, underscoring the intricate nature of intramolecular dynamics. By leveraging multifrequency nonlinear mode coupling, we induce a distinct chaotic response through strong external driving.

## 4 Conclusion

Although soliton molecules have been discovered in ultrafast lasers for over 30 years, the dynamical processes that govern them remain poorly understood, primarily due to the absence of a universal physical model that could describe their intramolecular motion. In this study, we first introduce the concept of a driven damped harmonic oscillator to the realm of soliton molecules dynamics, revealing a well-defined resonant response in intrapulse separation characterized by the universal Duffing model. This approach offers a critical framework for investigating the nonlinear mechanisms underlying soliton interactions within the laser system.

Our findings contribute to the fundamental understanding of multisoliton physics within a broad context and offer new insights into the buildup mechanisms and interactions of multisoliton states across a wide range of physical systems, including Mamyshev oscillators and passive optical resonators. Additionally, our work is expected to inspire further research into questions, such as the symmetry-breaking dynamics of internal motion in vector soliton molecules and marginal stability within the context of symmetry-breaking dynamics of vector dissipative solitons,[60] the nature of eigenfrequencies in trisoliton systems,[61] the potential existence of multiple eigenfrequencies, and whether their nonlinear resonance responses reveal a more

intricate framework. Notably, resonant excitation provides a general approach to generating breathers, laying the groundwork for investigating the fractal dynamics within intramolecular dynamics.[62] For practical applications, ultrafine scanning of temporal separations of ultrashort laser pulses, ranging from a few femtoseconds to hundreds of femtoseconds, shows great potential in areas requiring high detection sensitivity.[63]

## Disclosures

The authors declare no conflicts of interest.

## Code and Data Availability

The data that support the findings of this study are available from the corresponding authors on reasonable request.

### *Acknowledgments*

This work was supported by the National Natural Science Foundation of China (Grant Nos. 62405128, 61827821, 62220106006, and 62361136584); the China Postdoctoral Science Foundation (Grant No. 2024M751299); the Shenzhen Science and Technology Program (Grant Nos. SGDX20211123114001001 and JSGGKOTD20221101115656030); the Guangdong Basic and Applied Basic Research Foundation (Grant No. 2021B1515120013); and the Southern University of Science and Technology High Level of Special Funds (Grant Nos. G030230001 and G03034K004).

### *References*

1. S. H. Strogatz, *Nonlinear Dynamics and Chaos: With Applications to Physics, Biology, Chemistry, and Engineering*, CRC Press (2018).
2. M. Kauranen and A. V. Zayats, "Nonlinear plasmonics," *Nat. Photonics* **6**(11), 737–748 (2012).
3. A. H. Nayfeh and D. T. Mook, *Nonlinear Oscillations*, John Wiley & Sons (2008).
4. E. Ott, C. Grebogi, and J. A. Yorke, "Controlling chaos," *Phys. Rev. Lett.* **64**(11), 1196–1199 (1990).
5. G. M. Whitesides and B. Grzybowski, "Self-assembly at all scales," *Science* **295**(5564), 2418–2421 (2002).
6. M. W. Hirsch, S. Smale, and R. L. Devaney, *Differential Equations, Dynamical Systems, and an Introduction to Chaos*, Academic Press (2013).
7. Q. P. Unterreithmeier, T. Faust, and J. P. Kotthaus, "Damping of nanomechanical resonators," *Phys. Rev. Lett.* **105**(2), 027205 (2010).
8. N. I. Zheludev and Y. S. Kivshar, "From metamaterials to metadevices," *Nat. Mater.* **11**(11), 917–924 (2012).
9. A. Eichler et al., "Nonlinear damping in mechanical resonators made from carbon nanotubes and grapheme," *Nat. Nanotechnol.* **6**(6), 339–342 (2011).
10. J. M. Dudley, G. Genty, and S. Coen, "Supercontinuum generation in photonic crystal fiber," *Rev. Mod. Phys.* **78**(4), 1135–1184 (2006).
11. F. T. Arecchi, S. Boccaletti, and P. L. Ramazza, "Pattern formation and competition in nonlinear optics," *Phys. Rep.* **318**(1–2), 1–83 (1999).
12. Y. V. Kartashov, B. A. Malomed, and L. Torner, "Solitons in nonlinear lattices," *Rev. Mod. Phys.* **83**(1), 247–305 (2011).
13. W Jia et al., "Intracavity spatiotemporal metasurface," *Adv. Photonics* **5**(2), 026002 (2023).
14. J. Zou et al., "3.6 W compact all-fiber $Pr^{3+}$-doped green laser at 521 nm," *Adv. Photonics* **4**(5), 056001 (2022).
15. P. M. Paul et al., "Observation of a train of attosecond pulses from high harmonic generation," *Science* **292**(5522), 1689–1692.
16. P. Del'Haye et al., "Optical frequency comb generation from a monolithic microresonator," *Nature* **450**(7173), 1214–1217 (2007).
17. W. Wang, L. Wang, and W. Zhang, "Advances in soliton microcomb generation," *Adv. Photonics* **2**(3), 034001 (2020).
18. M. Yu et al., "Mode-locked mid-infrared frequency combs in a silicon microresonator," *Optica* **3**(8), 854–860 (2016).
19. H. Zhang et al., "The dissipative Talbot soliton fiber laser," *Sci. Adv.* **10**(11), eadl2125 (2024).
20. J. Peng et al., "Modulation instability in dissipative soliton fiber lasers and its application on cavity net dispersion measurement," *J. Lightwave Technol.* **30**(16), 2707–2712 (2012).
21. N. N. Akhmediev, A. Ankiewicz, and J. M. Soto-Crespo, "Multisoliton solutions of the complex Ginzburg-Landau equation," *Phys. Rev. Lett.* **79**(21), 4047–4051 (1997).
22. D. Y. Tang et al., "Observation of bound states of solitons in a passively mode-locked fiber laser," *Phys. Rev. A* **64**(3), 033814 (2001).
23. J. M. Soto-Crespo et al., "Soliton complexes in dissipative systems: vibrating, shaking, and mixed soliton pairs," *Phys. Rev. E* **75**(1), 016613 (2007).
24. L. M. Zhao et al., "Bound states of gain-guided solitons in a passively mode-locked fiber laser," *Opt. Lett.* **32**(21), 3191–3193 (2007).
25. B. Cao et al., "Spatiotemporal mode-locking and dissipative solitons in multimode fiber lasers," *Light Sci. Appl.* **12**(1), 260 (2023).
26. S. Liu et al., "On-demand harnessing of photonic soliton molecules," *Optica* **9**(2), 240–250 (2022).
27. Y. Guo et al., "Unveiling the complexity of spatiotemporal soliton molecules in real time," *Nat. Commun.* **14**(1), 2029 (2023).
28. Y. Han et al., "Pure-high-even-order dispersion bound solitons complexes in ultra-fast fiber lasers," *Light Sci. Appl.* **13**(1), 101 (2024).
29. X. Hu et al., "Novel optical soliton molecules formed in a fiber laser with near-zero net cavity dispersion," *Light Sci. Appl.* **12**(1), 38 (2023).
30. Z. Z. Si et al., "Polarization-induced buildup and switching mechanisms for soliton molecules composed of noise-like-pulse transition states," *Laser Photonics Rev.* 2401019 (2024).
31. G. Herink et al., "Real-time spectral interferometry probes the internal dynamics of femtosecond soliton molecules," *Science* **356**(6333), 50–54 (2017).
32. K. Krupa et al., "Real-time observation of internal motion within ultrafast dissipative optical soliton molecules," *Phys. Rev. Lett.* **118**(24), 243901 (2017).
33. X. Liu, X. Yao, and Y. Cui, "Real-time observation of the buildup of soliton molecules," *Phys. Rev. Lett.* **121**(2), 023905 (2018).
34. Y. Zhou et al., "Buildup and dissociation dynamics of dissipative optical soliton molecules," *Optica* **7**(8), 965–972 (2020).
35. Y. Cui et al., "Dichromatic "breather molecules" in a mode-locked fiber laser," *Phys. Rev. Lett.* **130**(15), 153801 (2023).
36. D. Zou et al., "Quantum limited timing jitter of soliton molecules in a mode-locked fiber laser," *Opt. Express* **29**(21), 34590–34599 (2021).
37. D. Zou et al., "Quasi-period dynamics of soliton molecules: route to chaos and intrinsic frequency entrainment," *Ultrafast Sci.* **4**, 0061 (2024).
38. Y. Du et al., "Stable loosely bounded asymmetric soliton molecules in fiber lasers," *Phys. Rev. A* **104**(4), 043508 (2021).
39. J. Peng et al., "Breather molecular complexes in a passively mode-locked fiber laser," *Laser Photonics Rev.* **15**(7), 2000132 (2021).
40. X. Lu et al., "From breather soliton molecules to chaos in a laser cavity: the scenario of intermittent transitions," *Opt. Express* **32**(15), 26207–26216 (2024).
41. Y. Song et al., "Chaotic internal dynamics of dissipative optical soliton molecules," *Laser Photonics Rev.* **17**(8), 2300066 (2023).

42. F. Kurtz, C. Ropers, and G. Herink, "Resonant excitation and all-optical switching of femtosecond soliton molecules," *Nat. Photonics* **14**(1), 9–13 (2020).
43. C. Luo et al., "Real-time comprehensive control over soliton molecules enabled by physics-inspired searching," *Laser Photonics Rev.* **18**(12), 2401153 (2024).
44. L. Nimmesgern et al., "Soliton molecules in femtosecond fiber lasers: universal binding mechanism and direct electronic control," *Optica* **8**(10), 1334–1339 (2021).
45. Y. Liu et al., "Phase-tailored assembly and encoding of dissipative soliton molecules," *Light Sci. Appl.* **12**(1), 123 (2023).
46. M. Pang et al., "All-optical bit storage in a fibre laser by optomechanically bound states of solitons," *Nat. Photonics* **10**(7), 454–458 (2016).
47. W. Weng, R. Bouchand, and T. J. Kippenberg, "Formation and collision of multistability-enabled composite dissipative Kerr solitons," *Phy. Rev. X* **10**(2), 021017 (2020).
48. D. Zou et al., "Synchronization of the internal dynamics of optical soliton molecules," *Optica* **9**(11), 1307–1313 (2022).
49. U. Fano, "Effects of configuration interaction on intensities and phase shifts," *Phys. Rev.* **124**, 1866–1878 (1961).
50. R. Weill et al., "Noise-mediated Casimir-like pulse interaction mechanism in lasers," *Optica* **3**(2), 189–192 (2016).
51. M. H. J. De Jong et al., "Mechanical overtone frequency combs," *Nat. Commun.* **14**(1), 1458 (2023).
52. H. A. Haus, "Mode-locking of lasers," *IEEE J. Sel. Top. Quantum Electron.* **6**, 1173–1185 (2000).
53. T. Kaisar et al., "Nonlinear stiffness and nonlinear damping in atomically thin $MoS_2$ nanomechanical resonators," *Nano Lett.* **22**(24), 9831–9838 (2022).
54. A. Prosperetti, "Application of the subharmonic threshold to the measurement of the damping of oscillating gas bubbles," *J. Acoust. Soc. Amer.* **61**, 11–16 (1977).
55. X. Zhang et al., "From breather solitons to chaos in an ultrafast laser: the scenario of cascading short and long-period pulsations," *Chaos Solitons Fractals* **182**, 114841 (2024).
56. X. Wu et al., "Synchronization, desynchronization, and intermediate regime of breathing solitons and soliton molecules in a laser cavity," *Phys. Rev. Lett.* **131**(26), 263802 (2023).
57. M. T. Rosenstein, J. J. Collins, and C. J. De Luca, "A practical method for calculating largest Lyapunov exponents from small data sets," *Phys. D* **65**(1–2), 117–134 (1993).
58. J. M. Soto-Crespo and N. Akhmediev, "Soliton as strange attractor: nonlinear synchronization and chaos," *Phys. Rev. Lett.* **95**(2), 024101 (2005).
59. H. Kang et al., "Observation of optical chaotic solitons and modulated subharmonic route to chaos in mode-locked laser," *Phys. Rev. Lett.* **133**, 263801 (2024).
60. G. Xu et al., "Spontaneous symmetry breaking of dissipative optical solitons in a two-component Kerr resonator," *Nat. Commun.* **12**(1), 4023 (2021).
61. F. Xin et al., "Evidence of chaotic dynamics in three-soliton collisions," *Phys. Rev. Lett.* **127**(13), 133901 (2021).
62. X. Wu et al., "Farey tree and devil's staircase of frequency-locked breathers in ultrafast lasers," *Nat. Commun.* **13**(1), 5784 (2022).
63. J. A. Lang et al., "Controlling intracavity dual-comb soliton motion in a single-fiber laser," *Sci. Adv.* **10**(2), eadk229 (2024).



**Defeng Zou** received his PhD from Tianjin University (TJU) in 2023 and is currently working as a postdoctoral fellow in the Department of Electronic and Electrical Engineering at the Southern University of Science and Technology. His research interests include ultrafast lasers and soliton dynamics. He has received awards such as the Wang Daheng Optical Award and the Guo Guangcan Optical Award for Scientific and Technological Innovation from the Chinese Optical Society.

**Minglie Hu** received the BSc degree in electrical engineering from the School of Precision Instruments and Optoelectronics Engineering, Tianjin University, Tianjin, China, in 2000. He received the PhD degree in optical engineering from Tianjin University in 2005. He is now a professor at Tianjin University. His current research interests include mode-locking laser oscillators and amplifiers, fiber lasers, nonlinear and linear propagation in the photonic crystal fibers, and microstructure optical devices.

**Perry Ping Shum** is an SPIE Fellow. He received his BEng and PhD degrees in Electronic and Electrical Engineering from the University of Birmingham, UK, in 1991 and 1995, respectively. In 1999, he joined Nanyang Technological University. In 2020, he joined Southern University of Science and Technology. He has served as the Director of the Network Technology Research Centre and has also held the positions of founding Director of the OPTIMUS-Photonics Centre and founding Director of the Centre for Optical Fibre Technology. Prof. Shum has published over 400 papers and has an H-index of 70. He has served as chair, committee member, and international advisor for numerous international conferences. His research interests encompass laser technology, biophotonics, silicon photonics, and fiber-based devices.

Biographies of the other authors are not available.